BIJECTIONS FOR GENERALIZED TAMARI INTERVALS VIA ORIENTATIONS

ÉRIC FUSY AND ABEL HUMBERT

Abstract. We present two bijections for generalized Tamari intervals, which were recently introduced by Préville-Ratelle and Viennot, and have been proved to be in bijection with rooted non-separable maps by Fang and Préville-Ratelle. Our first construction proceeds via separating decompositions on quadrangulations and can be seen as an extension of the Bernardi-Bonichon bijection between Tamari intervals and minimal Schnyder woods. Our second construction directly exploits the Bernardi-Bonichon bijection and the point of view of generalized Tamari intervals as a special case of classical Tamari intervals (synchronized intervals); it yields a trivariate generating function expression that interpolates between generalized Tamari intervals and classical Tamari intervals.

1. Introduction

The ν-Tamari lattice $\mathrm{Tam}(\nu)$ (for ν an arbitrary directed walk with steps in $\{N, E\}$) has been recently introduced by Préville-Ratelle and Viennot [24], and further studied in [11, 12], with connections to geometric combinatorics. It is a lattice on the set of directed walks weakly above ν and with same endpoints as ν, and it generalizes the Tamari lattice [26] (in size n, case where $\nu = (NE)^n$) and the m-Tamari lattices [2] (in size n, case where $\nu = (NE^m)^n$).

The enumeration of intervals (i.e., pairs formed by two elements x, x' with $x \leq x'$) in Tamari lattices has attracted a lot of attention [13, 7, 6], due in particular to their (conjectural) connections to dimensions of diagonal coinvariant spaces [2], and to their bijective connections to planar maps [4], as well as intriguing symmetry properties [22, 14]. Regarding ν-Tamari lattices, if we let $\mathcal{I}_\nu$ be the set of intervals in $\mathrm{Tam}(\nu)$, then it has recently been shown by Fang and Préville-Ratelle [16] that $\mathcal{G}_n := \cup_{\nu\in\{N,E\}^n}\mathcal{I}_\nu$ (generalized Tamari intervals of size n) is in bijection with the set $\mathcal{N}_n$ of rooted non-separable maps[1] with $n+2$ edges, and more precisely that $\mathcal{G}_{i,j} := \sum_{\nu\in\mathfrak{S}(E^iN^j)}\mathcal{I}_\nu$ is in bijection with the set $\mathcal{N}_{i,j}$ of rooted non-separable maps with $i+2$ vertices and $j+2$ faces (it is known [28, 10] that $|\mathcal{N}_n| = \frac{2(3n+3)!}{(n+2)!(2n+3)!}$ and $|\mathcal{N}_{i,j}| = \frac{(2i+j+1)!(2j+i+1)!}{(i+1)!(j+1)!(2i+1)!(2j+1)!}$). They have a first recursive bijection based on parallel decompositions with a catalytic variable, and then make the bijection more explicit via certain auxiliary labeled trees.

By a classical correspondence [9, Section 7], $\mathcal{N}_{i,j}$ is in bijection with the set $\mathcal{Q}_{i,j}$ of rooted bicolored quadrangulations with $i+2$ black vertices and $j+2$ white vertices (a quadrangulation is a simple map with all faces of degree 4, bicolored means that vertices

[1] A *map* is a connected multigraph embedded in the plane up to continuous deformation, a *rooted map* is a map with a marked corner incident to the outer face, and a map is called *non-separable* (or 2-connected) if it is either the loop-map, or is loopless and $M\backslash v$ is connected for every vertex $v \in M$.

are black or white so that all edges connect vertices of different color, and the vertex at the root-corner is black).

In this article, we give two new bijections between $\mathcal{G}_{i,j}$ and $\mathcal{Q}_{i,j}$. Each one relies on seeing $\mathcal{G}_{i,j}$ as included in a certain superfamily, and specializing a bijection involving oriented maps. In our first bijection (Section 3) we see $\mathcal{G}_{i,j}$ as a subfamily of non-intersecting triples of lattice walks (a so-called Baxter family) and specialize a bijection (closely related to the one in [20] and also to a recent bijection by Kenyon et al. [21]) with so-called separating decompositions on rooted quadrangulations. In our second bijection (Section 4) we see $\mathcal{G}_{i,j}$ as a subfamily of classical Tamari intervals of size $i+j+1$ (synchronized intervals), to which we apply the Bernardi-Bonichon bijection [4] (which maps Tamari intervals to minimal Schnyder woods on rooted triangulations) combined with a bijection [5] to certain tree-structures on which we can characterize the property of being synchronized.

Several parameters can be tracked by the first construction, which gives a model of maps for intervals in the m-Tamari lattices, and reveals certain symmetry properties on $\mathcal{G}_{i,j}$. The second construction yields a trivariate generating function expression (Corollary 2) that interpolates between the bivariate generating function of generalized Tamari intervals and the univariate generating function of classical Tamari intervals.

2. The ν-Tamari lattice, and generalized Tamari intervals

We recall [24] the definitions of ν-Tamari lattices and intervals, and how they relate to the classical Tamari lattice. We consider walks in $\mathbb{N}^2$ starting at the origin and having steps North or East (these can be identified with words on the alphabet $\{N, E\}$). For two such walks γ, γ', we say that γ' is *above* γ if γ and γ' have the same endpoint, and no East step of γ is strictly above the East step of γ' in the same vertical column. A Dyck walk of length $2n$ is thus a walk γ that is above $(NE)^n$. More generally, for ν a walk ending at (i, j), we let $\mathcal{W}_\nu$ be the set of walks above ν. For $\gamma \in \mathcal{W}_\nu$ and for $p = (x, y)$ a point on γ, we let $x' \geq x$ be the abscissa of the North step of ν from ordinate y to $y+1$ (with the convention that $x' = i$ if $y = j$), and we let $\ell(p) := x' - x$. If p is preceded by E and followed by N we let p' be the next point after p along γ such that $\ell(p') = \ell(p)$, and we let $\mathrm{push}_p(\gamma)$ be the walk γ' obtained from γ by moving the E preceding p to be just after p' (see Figure 1 for an example); we say that γ' covers γ. The Tamari lattice for ν is defined as $\mathrm{Tam}(\nu) = (\mathcal{W}_\nu, \leq)$ where $\leq$ is the transitive closure of the covering relation. The classical Tamari lattice Tam_n corresponds to the special case $\mathrm{Tam}_n = \mathrm{Tam}((NE)^n)$, and more generally for $m \geq 1$ the m-Tamari lattice $\mathrm{Tam}_n^{(m)}$ corresponds to the special case $\mathrm{Tam}_n^{(m)} = \mathrm{Tam}((NE^m)^n)$.

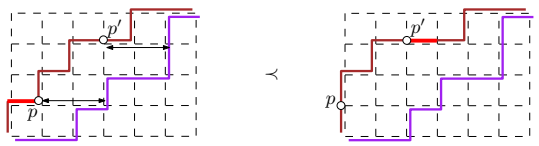

FIGURE 1. A covering relation in $\mathrm{Tam}(\nu)$ for $\nu = EENENEENNE$.

Interestingly, for ν of length n, $\mathrm{Tam}(\nu)$ can also be obtained as a sublattice of Tam_{n+1}. For $\gamma = E^{\alpha_0}NE^{\alpha_1}\cdots NE^{\alpha_n}$ a Dyck walk of length $2n$, the *canopy-word* of γ is the word $\mathrm{can}(\gamma) = (w_0, \ldots, w_n) \in \{0,1\}^{n+1}$ such that for $r \in [\![0, n]\!]$, $w_r = E$ if $\alpha_r = 0$ and $w_r = N$

if $\alpha_r \geq 1$ (note that we always have $w_0 = E$ and $w_n = N$). Then $\mathrm{Tam}(\nu)$ identifies to the sublattice of Tam_{n+1} induced by the Dyck walks whose canopy-word is equal to $E\nu N$.

Let $\mathcal{G}_{i,j}$ (resp. $\mathcal{G}_n$) be the set of triples (ν, γ, γ') such that $\gamma \leq \gamma'$ in $\mathrm{Tam}(\nu)$ and ν ends at (i, j) (resp. ν has length n). Elements of $\mathcal{G}_{i,j}$ (resp. $\mathcal{G}_n$) are called *generalized Tamari intervals* with endpoint (i, j) (resp. of size n). We now make two observations based on properties shown in [24] (each remark is associated with a bijection for $\mathcal{G}_{i,j}$ described later, respectively in Section 3 and Section 4, the second remark is also used in the bijection in [16]).

(i) Since $\gamma \leq \gamma'$ in $\mathrm{Tam}(\nu)$ implies that γ' is above γ, $\mathcal{G}_{i,j}$ is a subfamily of the family $\mathcal{R}_{i,j}$ of triples of walks (ν, γ, γ') all ending at (i, j) and such that γ' is above γ itself above ν.

(ii) On the other hand, let $\mathcal{I}_n$ be the set of intervals in Tam_n (classical Tamari intervals, on Dyck words). An interval $(\gamma, \gamma') \in \mathcal{I}_n$ is called *synchronized* if $\mathrm{can}(\gamma) = \mathrm{can}(\gamma')$. Let $\mathcal{S}_n \subset \mathcal{I}_n$ be the set of synchronized Tamari intervals of size n. Then the above sublattice characterization of $\mathrm{Tam}(\nu)$ implies that $\mathcal{G}_n$ is in bijection with $\mathcal{S}_{n+1}$. More generally, if we let $\mathcal{S}_{i,j}$ be the set of synchronized intervals such that the common canopy-word is in $\mathfrak{S}(E^{i+1}N^{j+1})$, then $\mathcal{G}_{i,j}$ is in bijection with $\mathcal{S}_{i,j}$.

3. Bijection using separating decompositions

Several bijections are known between $\mathcal{R}_{i,j}$ and other combinatorial families (which are called *Baxter families*, a survey is given in [19]). Our aim here is to pick one such bijection and show that it specializes nicely to the subfamily $\mathcal{G}_{i,j} \subset \mathcal{R}_{i,j}$. We pick the bijection from [20] for separating decompositions, but have to slightly modify it so that it specializes well (as we will see, our construction is also closely related to a recent bijection by Kenyon et al. [21]).

For $Q \in \mathcal{Q}_{i,j}$, we let s, s', t, t' be the outer vertices of Q in clockwise order around the outer face, with s the one at the root. A *separating decomposition* of Q is given by an orientation and coloration (blue or red) of each edge of Q such that all edges incident to s (resp. t) are ingoing blue (resp. ingoing red), and every vertex $v \notin \{s, t\}$ has outdegree 2 and satisfies the local conditions shown in Figure 2(a). An example of separating decomposition is given in Figure 2(b). It can be shown [15] that the blue edges form a spanning tree of $Q\backslash t$ and the red edges form a spanning tree of $Q\backslash s$. We let $\mathrm{Sep}_{i,j}$ be the set of pairs $S = (Q, X)$ where $Q \in \mathcal{Q}_{i,j}$, and X is a separating decomposition of Q. A separating decomposition is called *minimal* if it has no clockwise cycle.

A general property of outdegree-constrained orientations of planar maps [17] ensures that each rooted quadrangulation has a unique minimal separating decomposition, so that $\mathcal{Q}_{i,j}$ identifies to the subfamily of minimal separating decompositions from $\mathrm{Sep}_{i,j}$. We now recall the bijection Φ between $\mathrm{Sep}_{i,j}$ and $\mathcal{R}_{i,j}$ described in [20]. For $S \in \mathrm{Sep}_{i,j}$ we let T_{blue} be the blue tree, and let $v_0, \ldots, v_{j+1}$ be the white vertices ordered according to the first visit in a clockwise walk around T_{blue} starting at the root, and we let β_r be the number of ingoing red edges at v_{r+1}, for $r \in [\![0, j]\!]$.

Then $\Phi(S)$ is the triple of walks $(\gamma_{\mathrm{low}}, \gamma_{\mathrm{mid}}, \gamma_{\mathrm{up}})$ (written here as binary words) obtained as follows: the walk γ_{low} is obtained from a clockwise walk around T_{blue}, where we write an N each time —except for the last two occurences— we follow an edge $\circ - \bullet$ getting closer to the root and write an E each time we follow an edge $\circ - \bullet$ away from the root; the walk γ_{mid} is obtained from a clockwise walk around T_{blue}, where we write an N each time —except for the first and last occurence— we follow an edge $\bullet - \circ$ away

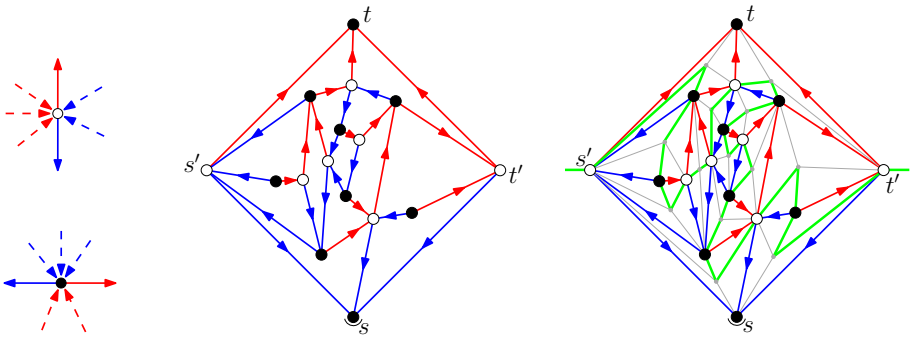

(a) (b) (c)

FIGURE 2. (a) Local rule of separating decompositions for vertices not in $\{s,t\}$. (b) A separating decomposition. (c) The equatorial line (in green).

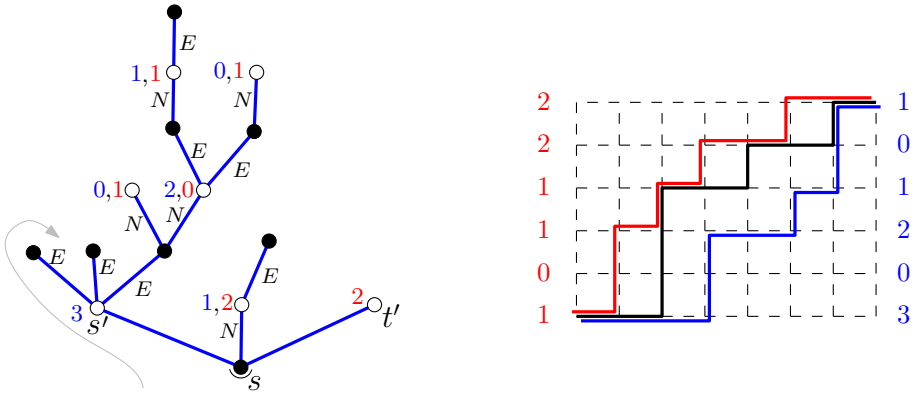

FIGURE 3. Left: the blue tree of the separating decomposition of Figure 2(b), with the indication of red and blue indegrees at white vertices. Right: the corresponding (by Φ') triple of walks.

from the root and write an E each time we follow an edge $\bullet - \circ$ getting closer to the root; the walk γ_{up} is $E^{\beta_0}NE^{\beta_1}\dots NE^{\beta_j}$.

We slightly modify the mapping as follows (see Figure 3 for an example): $\Phi'(S)$ is the triple $(\gamma_{\text{low}}, \gamma_{\text{mid}}, \gamma_{\text{up}})$ of walks where γ_{mid} and γ_{up} are obtained as above, and $\gamma_{\text{low}} = E^{\alpha_0}NE^{\alpha_1}\dots NE^{\alpha_j}$, with α_r the number of ingoing blue edges at v_r for $r \in [\![0,j]\!]$.

Theorem 1. *For $i,j \geq 0$, the mapping Φ' is a bijection between $\text{Sep}_{i,j}$ and $\mathcal{R}_{i,j}$. In addition, for $S \in \text{Sep}_{i,j}$, S is minimal iff $\Phi'(S) \in \mathcal{G}_{i,j}$, hence Φ' specializes into a bijection between $\mathcal{Q}_{i,j}$ and $\mathcal{G}_{i,j}$.*

The proof is delayed to Section 5. In the rest of the section we show some further properties of the bijection Φ' and their consequences, and the link to a recent bijection of Kenyon et al. [21].

Further parameter-correspondence. For $(\gamma_{\text{low}}, \gamma_{\text{mid}}, \gamma_{\text{up}}) \in \mathcal{R}_{i,j}$, a value $r \in [\![1, j]\!]$ is called a *level-value of type* (p, q) if $\beta_{r-1} = p$ and $\alpha_r = q$. On the other hand, for $Q \in \text{Sep}_{i,j}$, an inner white vertex is said to be *of type* (p, q) if it has p ingoing red edges and q ingoing blue edges. Then clearly in the bijection Φ', α_0 is mapped to the degree of s' minus 2, β_j is mapped to the degree of t' minus 2, and each level-value in $[\![1, j]\!]$ corresponds to an inner white vertex of the same type.

From this parameter-correspondence we can see that our bijection for $\mathcal{G}_{i,j}$ differs (under the classical correspondence of $\mathcal{N}_{i,j}$ with $\mathcal{Q}_{i,j}$) from the one in [16]. Indeed, in their bijection the parameter α_0 corresponds to the length (minus 1) of the leftmost branch in their labelled DFS trees. But that parameter does not correspond to a face-degree (e.g. for one of the two faces adjacent to the root-edge) nor to a vertex-degree (e.g. for one of the two extremities of the root-edge) in the associated rooted non-separable map.

A model of maps for intervals in $\text{Tam}_n^{(m)}$**.** For $m \geq 1$, we let $\mathcal{Q}_n^{(m)}$ be the subfamily of $\mathcal{Q}_{mn,n}$ where each inner white vertex has m ingoing blue edges in the minimal separating decomposition, and s' has no ingoing blue edge. Then Φ' specializes into a bijection between $\mathcal{Q}_n^{(m)}$ and intervals of $\text{Tam}_n^{(m)}$. It is known [7] (extension of the formula for $m = 1$ discovered in [13]) that the number $I_n^{(m)}$ of intervals in $\text{Tam}_n^{(m)}$ is given by the beautiful formula

$$I_n^{(m)} = \frac{m+1}{n(mn+1)} \binom{(m+1)^2 n + m}{n-1}. \tag{1}$$

The family $\mathcal{Q}_n^{(1)}$ is in bijection (via contraction of the blue edges directed toward a white vertex [20, Section 5]) with rooted triangulations (simple planar maps with all faces of degree 3) with $n + 3$ vertices, endowed with their minimal Schnyder wood. Under this correspondence one can check that our bijection coincides with the one by Bernardi and Bonichon [4] (recalled and exploited in Section 4) between $\mathcal{I}_n$ and rooted triangulations with $n + 3$ vertices. Rooted triangulations with $n + 3$ vertices can then be bijectively enumerated (we will recall a correspondence to certain mobiles in Section 4), giving a bijective proof of (1) for the case $m = 1$. It would be interesting to provide a bijective proof of (1) working for all $m \geq 1$, based on such an approach (edge-contractions or similar operations applied to maps in $\mathcal{Q}_n^{(m)}$, so as to obtain maps or hypermaps amenable to bijective enumeration).

A more symmetric formulation of the bijection Φ'**.** We reformulate here the bijection Φ' in a more symmetric way (in terms of the roles played by blue and red edges). We recall from [18, 19] the notions of equatorial line and 2-book embedding of a separating decomposition $S = (Q, X)$. We let H be the map, called the *augmented map* of Q, obtained from Q as follows: in each inner face f of Q, insert a gray vertex connected by new edges to the 4 corners around f, then delete the edges of Q. Note that each edge of H corresponds to a corner in an inner face of Q; such a corner is called *bicolored* if the two edges delimiting the corner are of different colors (one is blue and one is red) and is called *unicolored* otherwise. The edges of H associated to bicolored (resp. unicolored) corners of Q are colored green (resp. gray). The local conditions of separating decompositions ensure that each inner vertex of Q has two bicolored corners, the outer vertices s', t' have one bicolored corner, and s, t have no bicolored corner. In addition it is easily checked that each inner face has two bicolored corners. Hence the

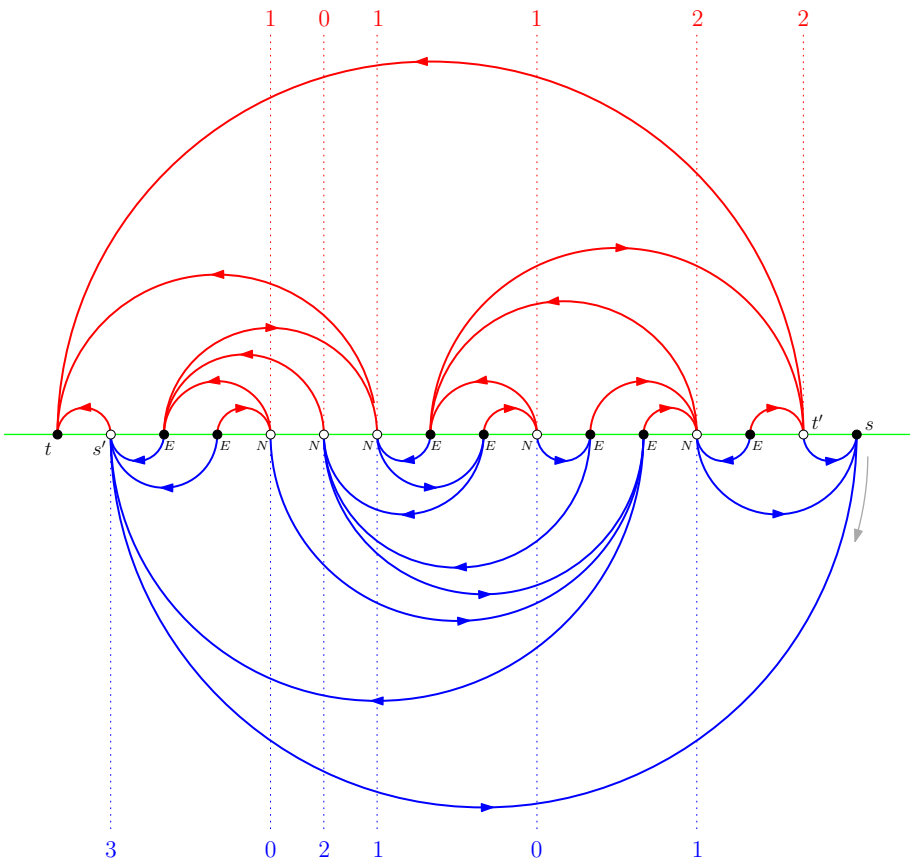

FIGURE 4. The 2-book embedding of the separating decomposition of Figure 2(b). The first-visit order of white vertices around the blue tree corresponds to the left-to-right order along the line, and the middle word (when applying Φ') is obtained by reading the inner vertices left to right along the line, writing E (resp. N) at every black (resp. white) vertex.

number of green edges incident to a vertex $v \in H$ is 0 if $v \in \{s, t\}$, is 1 if $v \in \{s', t'\}$, and is 2 otherwise. It is shown in Lemma 3.1 of [19] that the green edges actually form a simple path from s' to t' that visits all vertices of H except s and t; this path P is called the *equatorial line* of S, see Figure 2(c).

One can then stretch P into a horizontal line where the vertices of Q are equally spaced (with t as the left extremity and s as the right extremity) and planarly draw the blue (resp. red) edges of S as half-circles in the lower (resp upper) half-plane, see Figure 4. This canonical drawing is called the *2-book embedding* of S. It is shown in Theorem 2.14 of [18] (see also Proposition 3.3 in [19]) that the 2-book embedding of S satisfies the following so-called *alternating condition*: for all blue (resp. red) edges the right (resp. left) extremity is black. From this property and planarity (see the discussion on fingerprints in Section 3 of [19]), one can deduce that when applying the bijection Φ', the word corresponding to the middle walk exactly corresponds to the word read by

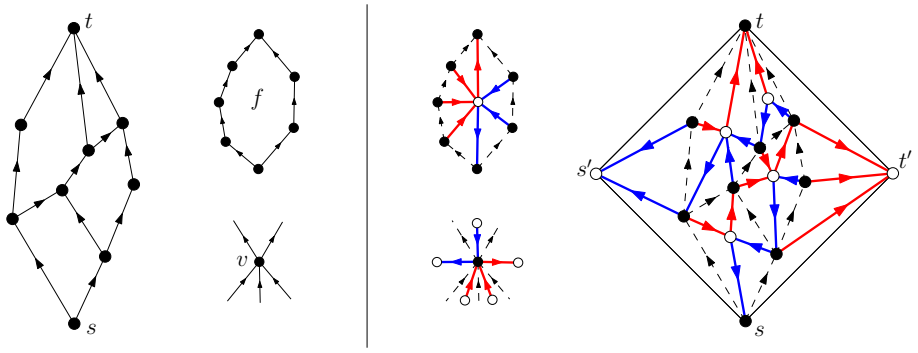

FIGURE 5. Left: a plane bipolar orientation B, with the conditions at inner faces and at non-pole vertices. Right: the corresponding separating decomposition $S = \iota(B)$.

traversing the line from left to right (excluding the outer vertices $\{s, t, s', t'\}$), writing E (resp. N) every time we meet a black (resp. white) vertex, see Figure 4. It also implies that the white vertices $v_0, \dots, v_{j+1}$ (ordered according to first visits in a clockwise walk around the blue tree starting at the root-corner) are ordered left-to-right along the line.

For $S \in \mathrm{Sep}_{i,j}$ we let $\tau(S)$ be the separating decomposition obtained as the half-turn rotation of S, i.e., the roles of s and t are exchanged and the colors are swapped. On the other hand for $R = (\gamma_{\mathrm{low}}, \gamma_{\mathrm{mid}}, \gamma_{\mathrm{up}}) \in \mathcal{R}_{i,j}$ we let $\tau(R)$ be the half-turn rotation of R, i.e., if $\mathrm{mir}(c_1, \dots, c_n) := (c_n \dots c_1)$ denotes the mirror of a word on $\{N, E\}$, then $\tau(R) := (\mathrm{mir}(\gamma_{\mathrm{up}}), \mathrm{mir}(\gamma_{\mathrm{mid}}), \mathrm{mir}(\gamma_{\mathrm{low}}))$. Clearly the symmetric reformulation of Φ' ensures that if $S \in \mathrm{Sep}_{i,j}$ is mapped by Φ' to $R \in \mathcal{R}_{i,j}$, then $\tau(S)$ is mapped to $\tau(R)$. Since τ is an involution on $\mathrm{Sep}_{i,j}$ that preserves the property of being minimal, we obtain (using Theorem 1):

Corollary 1. *For $R \in \mathcal{R}_{i,j}$ we have $\tau(R) \in \mathcal{G}_{i,j}$ iff $R \in \mathcal{G}_{i,j}$.*

To be precise, in our proof of the specialization part of Theorem 1 (in Section 5.2) we will use a characterization of elements of $\mathcal{G}_{i,j}$ in terms of a certain arc diagram representation (Lemma 2), and from this representation Corollary 1 already follows.

Link to a bijection by Kenyon et al. [21]**.** A *plane bipolar orientation* is a rooted map endowed with an acyclic orientation having a unique source s and a unique sink t both incident to the outer face, see Figure 5 left. It is known [15] that in a plane bipolar orientation every inner face has its incident edges partitioned into a non-empty interval of clockwise edges and a non-empty interval of counterclockwise edges —the face is said to be of type (p, q) if the first interval has length $p+1$ and the second interval has length $q+1$— and for every non-pole vertex (vertex $\notin \{s, t\}$) the incident edges are partitioned into a non-empty interval of ingoing edges and a non-empty interval of outgoing edges. We let $\mathcal{B}_{i,j}$ be the set of plane bipolar orientations with i non-pole vertices and j inner face, and let $\mathcal{B}_{i,j}[a, b]$ be the subset of those where the left (resp. right) outer boundary has length $a + 1$ (resp. $b + 1$). We let $\mathrm{Sep}_{i,j}[a, b]$ be the subset of $\mathrm{Sep}_{i,j}$ where s' has degree $a + 2$ and t' has degree $b + 2$. There is a direct bijection ι (illustrated in Figure 5)

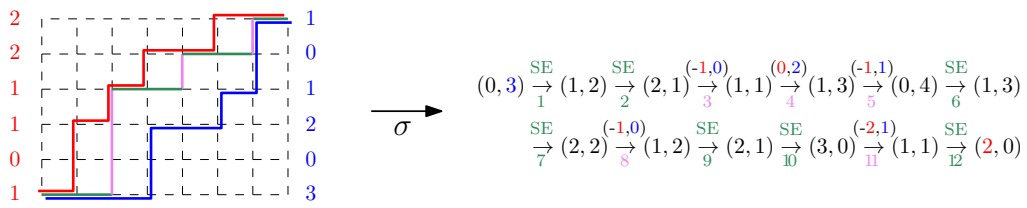

FIGURE 6. Left: a triple of walks in $\mathcal{R}_{7,5}[3,2]$ (the one obtained in Figure 3). Right: the corresponding (by σ) tandem walk in $\mathcal{W}_{7,5}[3,2]$.

from $\mathcal{B}_{i,j}[a,b]$ to $\mathrm{Sep}_{i,j}[a,b]$ where each vertex corresponds to a black vertex, and each inner face corresponds to an inner white vertex of the same type [15].

On the other hand, a *tandem walk* is a 2D walk where each step is either $(1,-1)$ (SE step) or a step of the form $(-p,q)$ for some $p,q \geq 0$. We let $\mathcal{W}_{i,j}[a,b]$ be the set of tandem walks of length $i+j$ with i SE steps, starting at $(0,a)$, ending at $(b,0)$ and staying in the quadrant $\mathbb{N}^2$. We let $\mathcal{R}_{i,j}[a,b]$ be the subset of elements in $\mathcal{R}_{i,j}$ where $\alpha_0 = a$ and $\beta_j = b$. We now recall a bijection σ from $\mathcal{R}_{i,j}[a,b]$ to $\mathcal{W}_{i,j}[a,b]$ recently described in [Sec 9.1][8] (where we slightly change the convention: the lower and upper walks are constructed line by line here, and column by column in [8]). For $R = (\gamma_{\mathrm{low}}, \gamma_{\mathrm{mid}}, \gamma_{\mathrm{up}}) \in \mathcal{R}_{i,j}[a,b]$, we let $n = i+j$ and let $u_1, \ldots, u_n$ be the successive steps in γ_{mid}. For $i \in [\![1,n]\!]$ we let s_i be a SE step if u_i is a horizontal step, and let $s_i = (-p,q)$ if u_i is the rth vertical step of γ_{mid} (with $r \in [\![1,j]\!]$), where $p = \beta_{r-1}$ and $q = \alpha_r$. Then $\sigma(R)$ is defined as the walk (in $\mathcal{W}_{i,j}[a,b]$) of length n starting at $(0,a)$ and with successive steps $s_1, \ldots, s_n$, see Figure 6 for an example. Combining the bijection Φ' with ι and σ, and with the parameter-correspondence of Φ' stated just after Theorem 1, we obtain:

Proposition 1. *The mapping $\Lambda := \sigma \circ \Phi' \circ \iota$ is a bijection from $\mathcal{B}_{i,j}[a,b]$ to $\mathcal{W}_{i,j}[a,b]$. Each non-pole vertex corresponds to a SE step, and each inner face of type (p,q) corresponds to a step $(-p,q)$.*

A bijection $\tilde{\Lambda}$ from $\mathcal{B}_{i,j}[a,b]$ to $\mathcal{W}_{i,j}[a,b]$ with the same parameter correspondence has been recently introduced by Kenyon et al. [21]. We recall now their bijection and then explain how it relates to Λ. For a bipolar orientation $B \in \mathcal{B}_{i,j}[a,b]$, the *rightmost tree* $T(B)$ of B is the spanning tree of B obtained by selecting every edge of B that is the rightmost ingoing edge at its end (see Figure 7 left). We let e' be the top-edge along the right outer boundary of B. For every edge e in $T(B)$, the *attached vertex* $v(e)$ is the end of e. For every edge e not in $T(B)$, the *attached face* $f(e)$ is the inner face on the right of e; note that e is the topleft edge of $f(e)$. Clearly every vertex different from s is the attached vertex of exactly one edge in $T(B)$, and every inner face is the attached face of exactly one edge not in $T(B)$. Note that a clockwise walk around $T(B)$ yields an ordered list $\gamma = (e_1, \ldots, e_{i+j+1})$ of the edges[2] of B: starting with $\gamma = \emptyset$, each time we walk along an edge e of $T(B)$ away from the root s we append e to γ, and each time we cross the outgoing half of an edge e not in $T(B)$ we append e to γ. Note that the last edge e_{i+j+1} has to be e'. Now the corresponding walk $\tilde{\Lambda}(B) \in \mathcal{W}_{i,j}[a,b]$ is the walk starting at $(0,a)$ and with successive steps $s_1, \ldots, s_{i+j}$ obtained as follows: for every $k \in [\![1, i+j]\!]$ if e_k is

[2]More generally this ordering of the edges can be considered for any rooted map endowed with a spanning tree, see [3] where it is exploited to get new bijective insights on the Tutte polynomial.

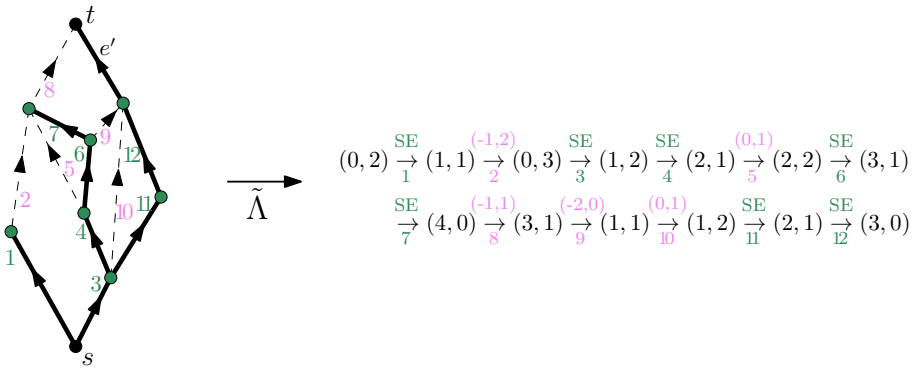

FIGURE 7. A plane bipolar orientation $B \in \mathcal{B}_{7,5}[2,3]$ and the corresponding tandem walk $\tilde{\Lambda}(B) \in \mathcal{W}_{7,5}[2,3]$.

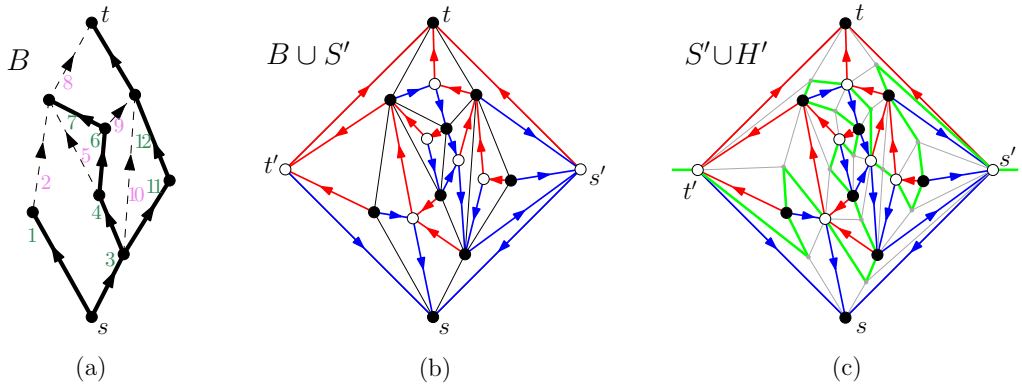

FIGURE 8. Link between the bijections $\tilde{\Lambda}$ and Λ via the equatorial line.

in $T(B)$ then s_k is a SE step, while if e_k is not in $T(B)$ then $s_k = (-p, q)$, where (p, q) is the type of the inner face $f(e_k)$, see Figure 7 for an example.

We now explain the link with our bijection Λ. First we recall the following bijection τ from $\mathcal{W}_{i,j}[a,b]$ to $\mathcal{W}_{i,j}[b,a]$: for a walk in $\mathcal{W}_{i,j}[a,b]$ with successive steps $s_1, \ldots, s_n$, its image by τ is the walk in $\mathcal{W}_{i,j}[b,a]$ with successive steps $\tilde{s}_n, \ldots, \tilde{s}_1$, where $\tilde{s}_k$ (for $k \in [\![1,n]\!]$) is a SE step if s_k is a SE step, and $\tilde{s}_k = (-q,p)$ if $s_k = (-p,q)$. In other words the mapping τ amounts to exchanging x and y and to reverse the time-direction, for example the tandem walk in Figure 6 is the image by τ of the tandem walk in Figure 7 (via the mapping σ^{-1} it is easy to see that the effect of τ is the half-turn rotation on triples of walks).

Let S' be obtained from B by applying the mapping ι using the mirror convention (compared to Figure 5) for the colors, see Figure 8(b). In other words, if we denote by $\mathrm{mir}(\cdot)$ the mirror according to a vertical axis (fixing s and t) then $S := \mathrm{mir}(S')$ is $\iota(\mathrm{mir}(B))$. Let Q' be the underlying quadrangulation of S', and let $H' = \mathrm{mir}(H)$ where H is the augmented map of S endowed with the equatorial line (green edges). For each

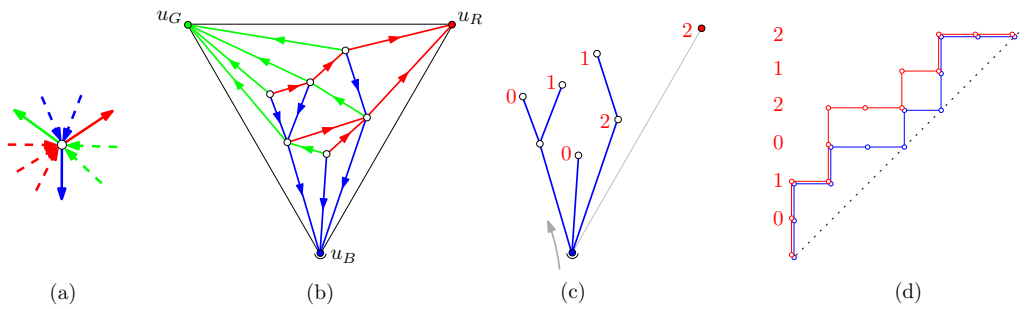

FIGURE 9. (a) Local rule for inner vertices in Schnyder woods. (b) A Schnyder wood with $n+3$ vertices ($n=6$). (c) The blue tree with the indication of red indegrees at vertices. (d) The corresponding pair of Dyck walks (the red one above the blue one) in $\mathcal{P}_n$.

edge e of B, we let $g(e)$ be the corresponding gray vertex of H' (vertex in the middle of e), and let $o(e)$ be the vertex of Q' that corresponds to the attached vertex $v(e)$ if $e \in T(B)$ and corresponds to the attached inner face $f(e)$ if $e \notin T(B)$. Then an easy case-by-case analysis ensures that for each $k \in [\![2, i+j]\!]$, along the equatorial line of H' (traversed from s' to t') the predecessor and successor of $g(e_k)$ are respectively $o(e_k)$ and $o(e_{k-1})$. This ensures that, along the equatorial line, the inner vertices of Q' are ordered as $o(e_{i+j}), o(e_{i+j-1}), \dots, o(e_1)$, which then easily implies that $\Lambda(\mathrm{mir}(B)) = \tau(\tilde{\Lambda}(B))$.

Remark. Another bijection from $\mathcal{B}_{i,j}$ to $\mathcal{R}_{i,j}$ is presented in [1, Sec 4.1]. It also relies on the rightmost tree (up to taking the dual bipolar orientation) and is closely related to the bijection $\sigma^{-1} \circ \Lambda$. But similarly as when taking Φ instead of Φ', one of the three walks (the upper one) differs.

4. Bijection using Schnyder woods

For T a rooted triangulation, the outer vertices are called u_B, u_G, u_R in clockwise order, with u_B the one incident to the root-corner. A *Schnyder wood* of T is an orientation and coloration (in blue, green or red) of every inner edge of T so that all edges incident to u_B, u_G, u_R are ingoing of color blue (resp. green, red), and every inner vertex has outdegree 3 and satisfies the local condition shown in Figure 9. A Schnyder wood induces a coloring of the corners: a corner at an inner vertex v receives the color of the 'opposite' outgoing edge at v, and a corner at an outer vertex v receives the color of v. It can be checked that around each inner face there is one corner in each color and these occur as blue, green, red in clockwise order. It is known that the local conditions of Schnyder woods imply that the graph in every color is a tree spanning all the internal vertices (plus the outer vertex of the same color, the root-vertex of the tree). A Schnyder wood is called *minimal* if it has no clockwise cycle. Any rooted triangulation has a unique minimal Schnyder wood [17].

Let $\mathcal{P}_n$ be the set of pairs (γ, γ') of Dyck paths of length $2n$ such that γ' is above γ. The Bernardi-Bonichon construction [4] starts from a triangulation with $n+3$ vertices endowed with a Schnyder wood, and outputs a pair $(\gamma, \gamma') \in \mathcal{P}_n$. Precisely (see Figure 9 for an example), we let T_{blue} be the blue tree of the Schnyder wood plus the outer edge

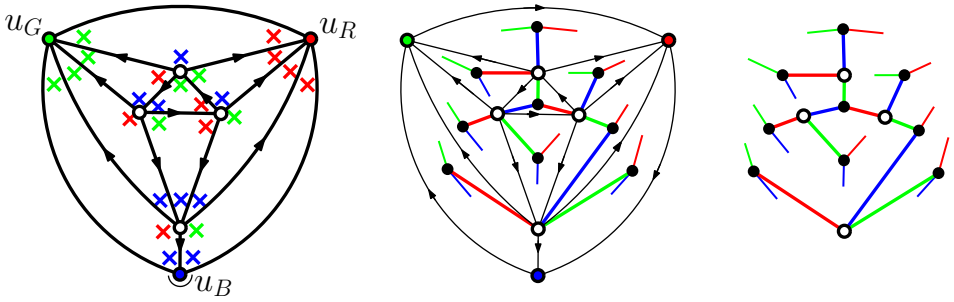

FIGURE 10. Left: A rooted triangulation endowed with its minimal Schnyder wood (colors are indicated at corners). Right: the corresponding 3-mobile.

$e' = \{u_B, u_R\}$, and let $v_0, \dots, v_n = u_R$ be the vertices of $T_{\text{blue}} \backslash \{u_B\}$ ordered according to the first visit in a clockwise walk around T_{blue} starting at u_B. Then γ is obtained as the contour walk of $T_{\text{blue}} \backslash e'$ and γ' is $NE^{\beta_1} NE^{\beta_2} \cdots NE^{\beta_n}$, with β_r the number of ingoing red edges at v_r for $r \in [\![1, n]\!]$. Bernardi and Bonichon show [4] that this gives a bijection between Schnyder woods on triangulations with $n+3$ vertices and $\mathcal{P}_n$; and they show that it specializes into a bijection between minimal Schnyder woods with $n+3$ vertices and $\mathcal{I}_n \subset \mathcal{P}_n$ (our Theorem 1 can be seen as an extension of this statement to separating decompositions, using the identification [20, Section 5] of Schnyder woods to separating decompositions where s' has blue indegree 0 and all inner white vertices have blue indegree 1).

On the other hand, minimal Schnyder woods are themselves known to be in bijection to certain tree structures [23, 5]. We will use here the bijection from [5]. A *3-mobile* is a (non-rooted) plane tree T where vertices have degree in $\{1, 3\}$ respectively called nodes and leaves, such that the nodes are colored black or white so that adjacent nodes have different colors, all leaves are adjacent to black nodes, and the edges are colored blue, green or red such that around each node the incident edges in clockwise order are blue, green and red. Additionally we require that there is at least one white node. In such a tree, an edge is called a *leg* if it is incident to a leaf and is called a *plain edge* otherwise. For $n \geq 1$ let $\mathcal{T}_n$ be the set of 3-mobiles with n white nodes. From a rooted triangulation M on $n+3$ vertices, endowed with its minimal Schnyder wood, one builds a 3-mobile $T \in \mathcal{T}_n$ as follows (see Figure 10): orient the outer cycle clockwise, insert a black vertex b_f in each inner face f of M, and then for each edge $e = u \to v$, with (f, f') the faces on the left and on the right of e, create a plain edge $\{u, b_f\}$ (if f is an inner face) and create a leg at $b_{f'}$ pointing (but not reaching) to v; and finally erase the outer vertices and all the edges of M. Each edge of T gets the color of the corresponding corner of M.

Composing both constructions, we get a bijection between $\mathcal{I}_n$ and $\mathcal{T}_n$. Let $(\gamma, \gamma') \in \mathcal{I}_n$, with $n \geq 1$. For $\binom{d}{c} \in \{\binom{N}{N}, \binom{E}{N}, \binom{E}{E}\}$ we say that a position $r \in [\![0, n]\!]$ is of type $\binom{d}{c}$ if there is c (resp. d) at position r in $\text{can}(\gamma)$ (resp. in $\text{can}(\gamma')$). Let $T \in \mathcal{T}_n$, with $n \geq 1$. A black node of T whose blue edge is a leg is said to be of type $\binom{N}{N}$ (resp. type $\binom{E}{E}$) if its red edge is a leg (resp. its green edge is a leg) and is said to be of type $\binom{E}{N}$ otherwise (only its blue edge is a leg).

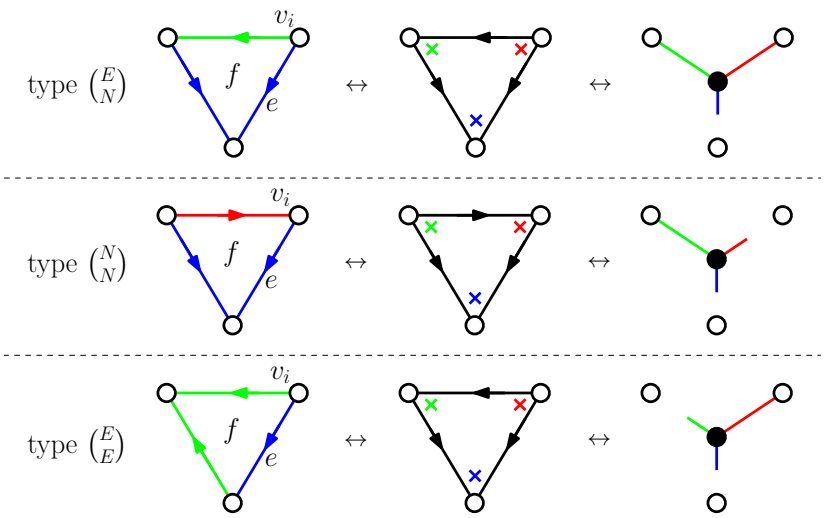

FIGURE 11. Left column: configuration of f for each of the possible types for position i. Right column: configuration at the corresponding black vertex in the 3-mobile.

Theorem 2. *Let $n \geq 1$. In the (composed) bijection between $\mathcal{I}_n$ and $\mathcal{T}_n$, each position $r \in [\![0, n]\!]$ corresponds to a black node of the same type.*

Proof. Let $(\gamma, \gamma') \in \mathcal{I}_n$, let S be the corresponding minimal Schnyder wood with $n+3$ vertices (with the notations T_{blue} and $v_0, \dots, v_n$ used in the Bernardi-Bonichon bijection, we take the convention that the outer edge $\{u_R, u_B\}$ is colored blue and directed toward u_B, and the outer edge $\{u_B, u_G\}$ is colored green and directed toward u_G), and let T be the corresponding 3-mobile. Let $r \in [\![0, n]\!]$. We denote by e the parent edge of v_r in T_{blue}, and by f the face on the right of e. By the Bernardi-Bonichon bijection, $\text{can}(\gamma')$ has E at position r iff there is no ingoing red edge at v_r, and $\text{can}(\gamma)$ has N at position r iff e comes just after a 'valley' in a clockwise walk around T_{blue}. From the local conditions of Schnyder woods, it is easy to see that each of the 3 possible types for r correspond to f being in each of the configuration shown in the left column of Figure 11. Let b_f be the black vertex of T that corresponds to f. From the mobile construction, it is easy to see that each of the configurations for f correspond to each of the configurations for b_f shown in the right column of Figure 11. This precisely corresponds to the given definitions of black vertices of types $\binom{E}{N}$, $\binom{N}{N}$, and $\binom{E}{E}$ respectively. □

Let $i, j, k \geq 0$, and $n = i + j + k + 1$. We denote by $a[i, j, k]$ the number of intervals in $\mathcal{I}_n$ having $i+1$ positions of type $\binom{E}{E}$, $j+1$ positions of type $\binom{N}{N}$ and k positions of type $\binom{E}{N}$, and we let $F(x, y, z) := \sum_{i,j,k} a[i, j, k] x^{i+1} y^{j+1} z^k$ be the associated generating function. Note that $F(x, y, 0) = \sum_{i,j} |\mathcal{S}_{i,j}| x^{i+1} y^{j+1} = \sum_{i,j} |\mathcal{G}_{i,j}| x^{i+1} y^{j+1}$.

Corollary 2. *The generating function $F \equiv F(x, y, z)$ is given by*

$$F = xR + yG + zRG - \frac{RG}{(1+R)(1+G)},$$

where R, G are the trivariate series (in x, y, z) specified by the system

$$\begin{cases} R &= (y + zR)(1 + R)(1 + G)^2, \\ G &= (x + zG)(1 + G)(1 + R)^2. \end{cases}$$

Before proving the corollary, we note that $F(x, y, 0)$ coincides (upon setting $G = u/(1-u)$ and $R = v/(1-v)$) with the known expression [10, Eq.2.3] of the bivariate series $\sum_{i,j} |\mathcal{Q}_{i,j}| x^{i+1} y^{j+1}$, and we recover $|\mathcal{G}_{i,j}| = |\mathcal{Q}_{i,j}|$ (we will also give a bijective argument at the end of the section); and $t + F(t, t, t)$ coincides (upon setting $G = R = \theta/(1 - \theta)$) with the known expression [27, Eq.4.9] of the series counting rooted simple triangulations by the number of vertices minus 2.

Proof. A *planted 3-mobile* T is defined similarly as a 3-mobile except that (exactly) one of the leaves is adjacent to a white node. This leaf is called the *root* of T, and its incident edge is called the *root-edge*. A planted 3-mobile is called *blue-rooted* (resp. *red-rooted*, *green-rooted*) if its root-edge is blue (resp. red, green). We keep the same definition of black nodes of types $\binom{E}{E}$, $\binom{N}{N}$, $\binom{E}{N}$ as for 3-mobiles. We let B, R, G be the trivariate (variables x, y, z) generating functions of blue-rooted, red-rooted, and green-rooted planted 3-mobiles, where x (resp. y, z) is dual to the number of black vertices of type $\binom{E}{E}$ (resp. type $\binom{N}{N}$, type $\binom{E}{N}$). A 2-levels decomposition at the root is translated into the following equation-system:

$$\begin{cases} B &= \big(B(1 + G) + x + zG\big)\big(B(1 + R) + y + zR\big), \\ R &= \big(B(1 + R) + y + zR\big)(1 + R)(1 + G), \\ G &= \big(B(1 + G) + x + zG\big)(1 + R)(1 + G). \end{cases}$$

In a 3-mobile T we note that the number of blue legs is one more than the number of blue plain edges[3]. Hence, by Theorem 2, $F = F_1 - F_2$ where F_1 is the trivariate series of 3-mobiles with a marked blue leg, and F_2 is the trivariate series of 3-mobiles with a marked blue plain edge. A decomposition at the marked blue leg gives $F_1 = xR + yG + zRG$, and a decomposition at the marked blue plain edge gives $F_2 = B(1+R)(1+G)$. We now simplify the equation-system by eliminating B. We look at the quantity $\frac{B(1+R)}{G}$, where we substitute B and G by their respective expressions in the equation-system. After simplification this gives $\frac{B(1+R)}{G} = \frac{B(1+R)+y+zR}{1+G}$, hence $B(1 + R) = yG + zRG$. Similarly looking at the quantity $\frac{B(1+G)}{R}$ we obtain $B(1 + G) = xR + zRG$. Substituting into the system we obtain

$$\begin{cases} B &= (1 + R)(x + zG)(1 + G)(y + zR), \\ R &= (y + zR)(1 + R)(1 + G)^2, \\ G &= (x + zG)(1 + G)(1 + R)^2, \end{cases}$$

and we have $F_2 = (x + zG)(y + zR)(1 + R)^2(1 + G)^2 = \frac{RG}{(1+R)(1+G)}$. □

A bijection between $\mathcal{G}_{i,j}$ and $\mathcal{Q}_{i,j}$ via mobiles. A 3-mobile (with at least one white node) is called *synchronized* if it has no black node of type $\binom{E}{N}$, i.e., every black node b having a blue leg is incident to (exactly) one other leg. If this other leg is red (resp. green) then b has type $\binom{N}{N}$ (resp. type $\binom{E}{E}$). We let $\mathcal{T}_{i,j}^{\text{syn}}$ be the set of synchronized

[3]An easy way to see it is via the associated minimal Schnyder woods S. Indeed in T there is a blue plain edge associated to every red edge (outgoing part) of S, and there is a blue leg associated to every blue edge (ingoing part) of S, plus an extra blue leg associated to the outer edge (u_B, u_R).

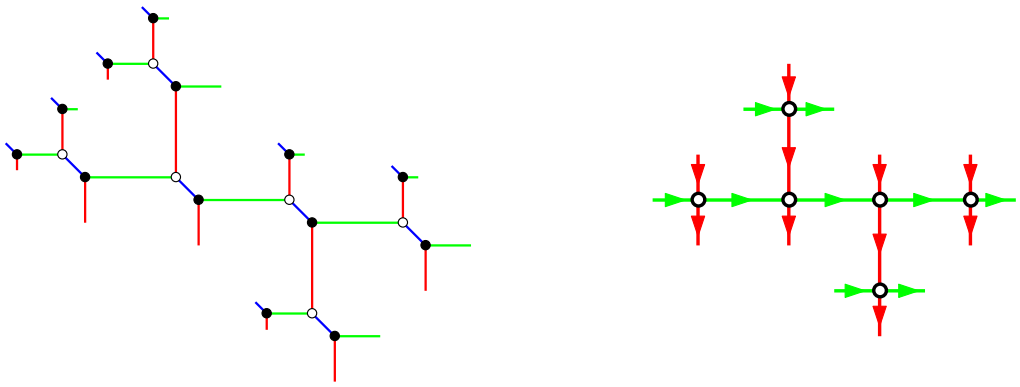

FIGURE 12. Left: a synchronized 3-mobile in $\mathcal{T}^{\mathrm{syn}}_{4,3}$. Right: the corresponding bicolored unrooted ternary tree in $\mathcal{U}_{4,3}$.

3-mobiles with $i+1$ black nodes of type $\binom{E}{E}$ and $j+1$ black nodes of type $\binom{N}{N}$. It follows from Theorem 2 that $\mathcal{T}^{\mathrm{syn}}_{i,j}$ is in bijection with $\mathcal{S}_{i,j}$, itself in bijection with $\mathcal{G}_{i,j}$.

An *unrooted ternary tree* is a plane tree where all vertices have degree in $\{1,4\}$, called respectively leaves and nodes. An unrooted ternary tree T is said to be *bicolored* if its edges are colored green or red and are oriented such that around each node the incident edges in clockwise order are ingoing red, outgoing green, outgoing red, and ingoing green. A leaf ℓ is called ingoing (resp. outgoing) if its incident edge e is outgoing (resp. ingoing), and is called red (resp. green) if e is red (resp. green). It is easy to see that T has as many red leaves that are outgoing as ingoing, and as many green leaves that are outgoing as ingoing. We let $\mathcal{U}_{i,j}$ be the set of bicolored unrooted ternary trees having $i+1$ outgoing red leaves and $j+1$ outgoing green leaves. A bijection between $\mathcal{Q}_{i,j}$ and $\mathcal{U}_{i,j}$ has been introduced in Section 2.3.3 of [25] and recovered in [5] (to obtain a ternary tree from a minimal separating decomposition, it actually uses the same local rules as those to obtain a 3-mobile from a minimal Schnyder wood).

Hence to derive another bijection between $\mathcal{G}_{i,j}$ and $\mathcal{Q}_{i,j}$ it remains to give a bijection between $\mathcal{T}^{\mathrm{syn}}_{i,j}$ and $\mathcal{U}_{i,j}$. The bijection, shown in Figure 12, is very simple. For $T \in \mathcal{T}^{\mathrm{syn}}_{i,j}$, the corresponding $U \in \mathcal{U}_{i,j}$ is obtained as follows: orient all the plain edges of T from black to white nodes, then contract the blue plain edges, and finally delete the two legs at each black node of type $\binom{N}{N}$ or $\binom{E}{E}$ (the black nodes of type $\binom{E}{E}$ become outgoing red leaves, those of type $\binom{N}{N}$ become outgoing green leaves).

5. Proof of Theorem 1

5.1. **Proof that Φ' is a bijection from $\mathrm{Sep}_{i,j}$ to $\mathcal{R}_{i,j}$.** We define a *blue-red arc diagram* as the figure obtained by concatenating $j+1$ horizontal segments $S_0,\dots,S_j$, where for $r \in [\![0,j]\!]$ the segment S_r is made of $\alpha_r \geq 0$ blue dots followed by $\mu_r \geq 0$ black dots followed by $\beta_r \geq 0$ red dots, and where in the lower part the blue dots are matched to the black dots (black dots closing the arcs) and in the upper part the black dots are matched to the red dots (black dots opening the arcs). We let $\mathcal{A}_{i,j}$ be the set of blue-red arc diagrams made of $j+1$ segments and having i black dots, see the right part of Figure 13. There is a straighforward bijection ξ between $\mathcal{A}_{i,j}$ and $\mathcal{R}_{i,j}$: for $A \in \mathcal{A}_{i,j}$ the corresponding triple of

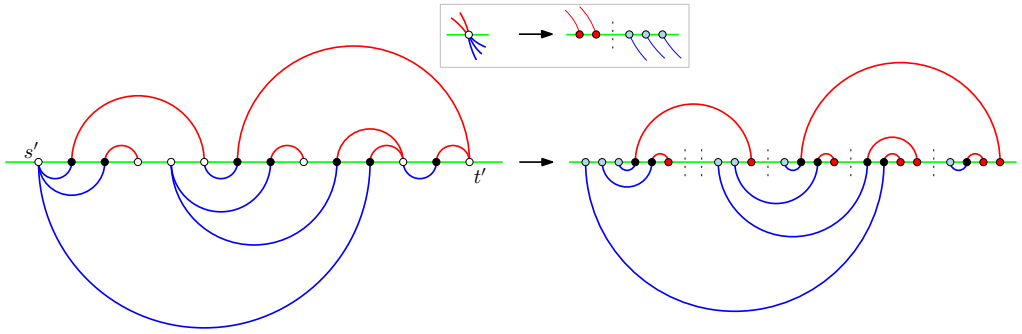

FIGURE 13. Left: the reduction of the 2-book embedding of Figure 4. Right: the corresponding blue-red arc diagram in $\mathcal{A}_{7,5}$.

walks $(\gamma_{\text{low}}, \gamma_{\text{mid}}, \gamma_{\text{up}}) \in \mathcal{R}_{i,j}$ is the one where γ_{low} (resp. γ_{mid}, γ_{up}) has α_r (resp. μ_r, β_r) East steps at height r for $r \in [\![0, j]\!]$. The property that γ_{mid} is above γ_{low} is equivalent to having $\sum_{k=0}^{r} \alpha_k \geq \sum_{k=0}^{r} \mu_k$ for all $r \in [\![0, j]\!]$, which is equivalent to the fact that blue dots can be matched to the black dots. Similarly the property that γ_{up} is above γ_{mid} is equivalent to the fact that the black dots can be matched to the red dots.

There is also an easy bijection χ from $\text{Sep}_{i,j}$ to $\mathcal{A}_{i,j}$. For $S \in \text{Sep}_{i,j}$, the *reduction* of the 2-book embedding of S is the figure S' obtained by erasing the vertices s and t and erasing all edges starting from a white vertex, see the left-part of Figure 13. The alternating property of 2-book embeddings implies that the diagrams S' are characterized by the following properties: they have black and white vertices aligned on a horizontal axis, red arcs in the upper half and blue arcs in the lower half (all connecting a black vertex to a white vertex), such that for every blue (resp. red) arc its right (resp. left) extremity is black, and such that every black vertex is incident to exactly one blue arc and exactly one red arc.

To recover the 2-book embedding from S', insert t (resp. s) as the left (resp. right) extremity on the line. Then for each white vertex w on the line, if w is "below" a blue arc a (i.e., a is the first arc crossed by a descending vertical line starting from w), then in the lower half-plane connect w to the (black) right end of a by a blue edge, and if w is not below an arc then connect w to s. Similarly, if w is "below" a red arc a (i.e., a is the first arc crossed by a rising vertical line starting from w), then in the upper half-plane connect w to the (black) left end of a by a red edge, and if w is not below an arc then connect w to t.

Then S' is easily turned into a blue-red arc diagram $A \in \mathcal{A}_{i,j}$ as shown in Figure 13. All transformations are easily reversible, so that χ is a bijection.

Finally we clearly have $\Phi' = \xi \circ \chi$, so that Φ' is a bijection from $\text{Sep}_{i,j}$ to $\mathcal{R}_{i,j}$.

5.2. **Proof that $S \in \text{Sep}_{i,j}$ is minimal iff $\Phi'(S) \in \mathcal{G}_{i,j}$.** In a blue-red arc diagram, a *Z-pattern* is a pair made of a blue arc a and a red arc a' such that the blue extremity of a is enclosed within a' and the red extremity of a' is enclosed within a, see Figure 14(a).

Our proof that $S \in \text{Sep}_{i,j}$ is minimal iff $\Phi'(S) \in \mathcal{G}_{i,j}$ relies on the two following lemmas.

Lemma 1. *Let $S \in \text{Sep}_{i,j}$ and let $A \in \mathcal{A}_{i,j}$ be the corresponding blue-red arc diagram (i.e., $A = \chi(S)$). Then S is minimal iff A has no Z-pattern.*

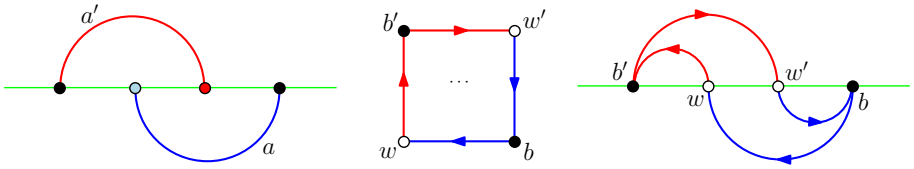

FIGURE 14. (a) A Z-pattern in a blue-red arc diagram (drawing only the two involved arcs and their extremities). (b) Situation for a clockwise 4-cycle in a separating decomposition. (c) Situation for a clockwise 4-cycle in the 2-book embedding of a separating decomposition (drawing only the four involved vertices and edges).

Proof. It is shown in Section 7 of [15] that, if S is not minimal, then it contains a clockwise 4-cycle C (not necessarily the contour of a face), and the local conditions (Figure 2(a)) imply that the colors are as shown in Figure 14(b). Then, in the 2-book embedding, the 4 edges of C are as shown in Figure 14(c). Hence the two arcs of A resulting from the two edges of C going out of a black vertex form a Z-pattern.

Conversely, assume A has a Z-pattern. A Z-pattern is called *minimum* if the distance along the line between its blue dot and its red dot is smallest possible. Let a, a' be a pair forming a minimum Z-pattern. Let $e = \{b, w\}$ and $e' = \{b', w'\}$ be the corresponding edges in the 2-book embedding of S. Let e'_1 be the outgoing red edge of w and let $\tilde{b}$ be its black extremity. Assume $\tilde{b} \neq b'$. Then the outgoing red edge e'_2 of $\tilde{b}$ is enclosed within e', hence it ends between w and w' (w excluded). Let a'_2 be the arc of A that corresponds to e_2. Then clearly the pair of arcs a, a'_2 forms a Z-pattern in A, contradicting the fact that the pair a, a' is minimum. Hence e'_1 ends at b'. Similarly, the outgoing blue edge of w' has to end at b. Hence the vertices b, w, b', w' form a clockwise 4-cycle, so that S is not minimal. □

Lemma 2. *Let $R = (\gamma_{\text{low}}, \gamma_{\text{mid}}, \gamma_{\text{up}}) \in \mathcal{R}_{i,j}$ and let $A \in \mathcal{A}_{i,j}$ be the corresponding blue-red arc diagram (i.e., $R = \xi(A)$). Then $R \in \mathcal{G}_{i,j}$ iff A has no Z-pattern.*

Proof. The *modified arc diagram* $\tilde{A}$ of A is the same as A except that the arcs in the upper part match the blue dots to the red dots instead of matching the black dots to the red dots, see Figure 15. Let $b_1, \dots, b_i$ be the blue dots of $\tilde{A}$ ordered from left to right, and let $\nu := \gamma_{\text{low}}$. For $k \in [\![1, i]\!]$, let $U_k \in [\![0, j]\!]$ be the index of the segment containing the black dot matched with b_k, and let $V_k \in [\![0, j]\!]$ be the index of the segment containing the red dot matched with b_k, see the left part of Figure 15. The vectors $\vec{U} = (U_1, \dots, U_k)$ and $\vec{V} = (V_1, \dots, V_k)$ are the *bracket vectors* [11] of γ_{mid} and γ_{up} with respect to ν (compared to [11] we omit the fixed underlined entries). It is shown in Section 4 of [11] that $\gamma_{\text{mid}} \leq \gamma_{\text{up}}$ in $\text{Tam}(\nu)$ iff $\vec{U} \leq \vec{V}$ (component by component). Clearly this is equivalent to the fact that the modified arc diagram $\tilde{A}$ avoids the pattern shown in the right part of Figure 15.

Assume $R \notin \mathcal{G}_{i,j}$, so that $\tilde{A}$ contains a pattern as in the right part of Figure 15. In this pattern let d_1, d_2, d_3 be the blue dot, red dot and black dot, let $a'' = (d_1, d_2)$ be the gray arc above and $a = (d_1, d_3)$ the blue arc below. Let E be the part of the line strictly between d_1 and d_2, and let $n_{\text{blue}}, n_{\text{black}}, n_{\text{red}}$ be respectively the numbers of blue dots,

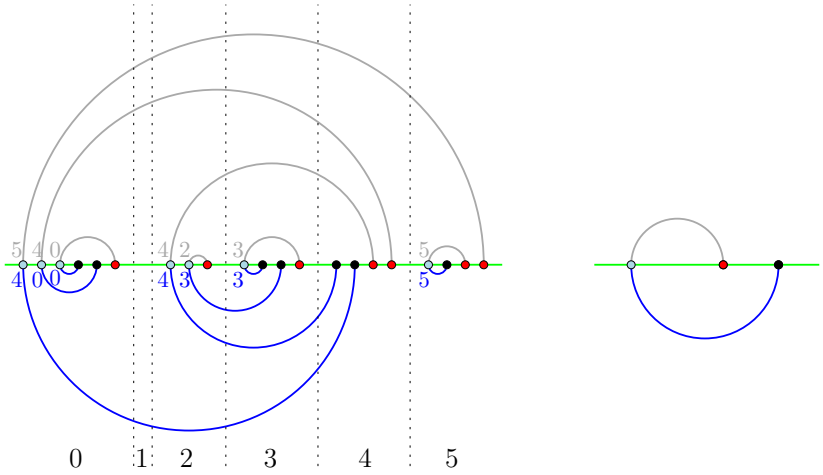

FIGURE 15. Left: the modified arc diagram of the blue-red arc diagram shown in the right part of Figure 13, which itself corresponds to the triple $R = (\gamma_{\text{low}}, \gamma_{\text{mid}}, \gamma_{\text{up}})$ shown in Figure 6. The bracket vectors of γ_{mid} and γ_{up} with respect to $\nu := \gamma_{\text{low}}$ are $\vec{U} = (4, 0, 0, 4, 3, 3, 5)$ and $\vec{V} = (5, 4, 0, 4, 2, 3, 5)$. We have $U_5 = 3 > 2 = V_5$, hence $\gamma_{\text{mid}} \not\leq \gamma_{\text{up}}$ in $\text{Tam}(\nu)$. Right: the pattern to be avoided to have $\gamma_{\text{mid}} \leq \gamma_{\text{up}}$ in $\text{Tam}(\nu)$.

black dots, and red dots in E. We have $n_{\text{blue}} = n_{\text{red}}$ since d_1 and d_2 are matched (for the upper diagram). We have $n_{\text{blue}} \geq n_{\text{black}}$ since in the lower diagram d_1 is matched to a black dot that is on the right of d_2. Hence $n_{\text{red}} \geq n_{\text{black}}$. In other word, in $E \cup d_2$ we have more red dots than black dots. This implies that, in the upper diagram of A, there is a red dot in $E \cup d_2$ that is matched to a black dot on the left of d_1. Hence, if we let a' be the arc formed by this matched pair, then the pair a, a' is a Z-pattern in A.

Assume now that A contains a Z-pattern, and let a, a' be a pair of arcs forming a minimum Z-pattern. We denote by d_1 the blue extremity of a, by d_2 the red extremity of a', and by E the part of the line strictly between d_1 and d_2. Let $n_{\text{blue}}, n_{\text{black}}, n_{\text{red}}$ be respectively the numbers of blue dots, black dots, and red dots in E. The fact that the pattern is minimum easily implies that there is no arc (neither in the upper nor in the lower diagram) starting from E and ending outside of E. Hence $n_{\text{blue}} = n_{\text{black}} = n_{\text{red}}$, so that in the upper diagram of $\tilde{A}$, d_1 has to be matched with a red dot belonging to $E \cup d_2$. Clearly this arc a'' together with a form a pattern as in the right part of Figure 15, hence $R \notin \mathcal{G}_{i,j}$. □

Acknowledgement. The authors thank Frédéric Chapoton, Guillaume Chapuy, Wenjie Fang and Mathias Lepoutre for interesting discussions. ÉF is supported by ANR-16-CE40-0009-01 "GATO", AH is supported by ERC-2016-STG 716083 "CombiTop".

REFERENCES

[1] Albenque M. and Poulalhon D., *Generic method for bijections between blossoming trees and planar maps*, Electron. J. Comb. **22** (2015), paper P2.38.

[2] Bergeron F. and Préville-Ratelle L.-F., *Higher trivariate diagonal harmonics via generalized Tamari posets*, J. Comb. **3** (2012), 317–341.
[3] Bernardi O. *Tutte polynomial, subgraphs, orientations and sandpile model: new connections via embeddings*, Electron. J. Comb. **15**(1) (2008), R109.
[4] Bernardi O. and Bonichon N., *Intervals in Catalan lattices and realizers of triangulations*, J. Combin. Theory Ser. A **116** (2009), 55–75.
[5] Bernardi O. and Fusy É., *A bijection for triangulations, quadrangulations, pentagulations, etc.*, J. Combin. Theory Ser. A **119** (2012), 218–244.
[6] Bousquet-Mélou M., Chapuy G., and Préville-Ratelle L.-F., *The representation of the symmetric group on m-Tamari intervals*, Adv. Math. **247** (2013), 309–342.
[7] Bousquet-Mélou M., Fusy É., and Préville-Ratelle L.-F., *The number of intervals in the m-Tamari lattices*, Electron. J. Combin. **18** (2012) paper 31.
[8] Bousquet-Mélou M., Fusy É., and Raschel K., *Plane bipolar orientations and quadrant walks*, arXiv preprint arXiv:1805.03566, 2019.
[9] Brown, W. G., *Enumeration of quadrangular dissections of the disk*, Canad. J. Math. **17** (1965), 302–317.
[10] Brown W. G. and Tutte W. T., *On the enumeration of rooted non-separable planar maps*, Canad. J. Math. **16** (1964), 572–577.
[11] Ceballos C., Padrol A., and Sarmiento C., *The ν-Tamari lattice as the rotation lattice of ν-trees*, arXiv preprint arXiv:1805.03566, 2018.
[12] ———, *Geometry of ν-Tamari lattices in types A and B*, Trans. Amer. Math. Soc. **371** (2019), 2575–2622.
[13] Chapoton F., *Sur le nombre d'intervalles dans les treillis de Tamari*, Sém. Lothar. Combin. **55** (2006), paper 36.
[14] Chapoton F., *Une note sur les intervalles de Tamari*, Ann. Math. Blaise Pascal **25**(2) (2018), 299–314.
[15] De Fraysseix H., Ossona de Mendez P., and Rosenstiehl P., *Bipolar orientations revisited*, Discrete Appl. Math. **56** (1995), 157–179.
[16] Fang W. and Préville-Ratelle L.-F., *The enumeration of generalized Tamari intervals*, European J. Combin. **61** (2017), 69–84.
[17] Felsner S., *Lattice structures from planar graphs*, Electron. J. Combin. **11** (2004), paper 15.
[18] Felsner S., Kappes S., Huemer C., and Orden D., *Binary Labelings for Plane Quadrangulations and their Relatives*, Discr. Math. and Theor. Comp. Sci. (DMTCS) **12**:3 (2010), 115–138.
[19] Felsner S., Fusy É., Noy M., and Orden D., *Bijections for Baxter families and related objects*, J. Combin. Theory Ser. A **118** (2011), 993–1020.
[20] Fusy É., Poulalhon D., and Schaeffer G., *Bijective counting of plane bipolar orientations and Schnyder woods*, European J. Combin. **30** (2009), 1646–1658.
[21] Kenyon, R., Miller, J., Sheffield, S., and Wilson, D. B., *Bipolar orientations on planar maps and* SLE_{12}, Ann. Probab. **47**(3) (2019), 1240–1269.
[22] Pons V., *The Rise-Contact involution on Tamari intervals*, Electron. J. Combin., **26**(2):P2.32, 2019
[23] Poulalhon, D. and Schaeffer, G., *Optimal coding and sampling of triangulations*, Algorithmica **46**(3-4) (2006), 505–527.
[24] Préville-Ratelle L.-F. and Viennot X., *An extension of Tamari lattices*, Trans. Amer. Math. Soc. **369**(7) (2017), 5219–5239.
[25] Schaeffer G., *Conjugaison d'arbres et cartes combinatoires aléatoires*, PhD thesis, Université de Bordeaux 1, 1998.
[26] Tamari D., *Monoïdes préordonnés et chaînes de Malcev*, PhD thesis, Université de Paris, 1951.
[27] Tutte W. T., *A census of planar triangulations*, Canad. J. Math. **14** (1962), 21–38.
[28] Tutte W. T., *A census of planar maps*, Canad. J. Math. **15** (1963), 249–271.

ÉF: CNRS/LIX, École Polytechnique, France
E-mail address: fusy@lix.polytechnique.fr

AH: IRIF, Université Paris-Diderot, France
E-mail address: ahumbert@irif.fr